International Journal of Modern Manufacturing Technologies
ISSN 2067–3604, Vol. XVI, No. 2 / 2024
https://doi.org/ 10.54684/ijmmt.2024.16.2.80

ENHANCING FORMABILITY OF AA6061 IN INCREMENTAL SHEET FORMING: EXPLORING PARAMETER EFFECTS ON FRACTURE DEPTH

Harit Raval[1], Viren Mevada[2]

[1,2]Department of Mechanical Engineering, Sardar Vallabhbhai National Institute of Technology, Surat, 395007Gujarat, India

Corresponding author: Harit Raval, hkr@med.svnit.ac.in

Abstract: AA6061's high strength and strain rate sensitivity in Incremental Sheet Forming (ISF) demand precise parameter control to prevent early fractures, especially at steep wall angles. Tool diameter influences the distribution of deformation forces, while spindle speed, step depth, and feed rate control the rate and extent of material deformation, collectively impacting the forming. This paper investigates the effect of these process parameters on the formability in terms of fracture depth. A statistical analysis is performed to identify the significant factors affecting forming depth. The main effect plot suggests that except the spindle speed, all three process parameters influence forming depth. However, the interaction plot reveals a more complex relationship, where step depth has a stronger effect on fracture depth, particularly at higher feed rates. These findings indicate that the interplay between these factors is crucial for determining optimal process parameters, where nearly 10% of increase in forming depth was achieved.

Keywords: incremental sheet forming, AA6061-T6, formability, forming depth, optimization.

1. INTRODUCTION

Incremental Sheet Forming (ISF) is a flexible manufacturing process where sheet metal is gradually formed into its final shape using a series of localized deformations. It offers advantages like rapid prototyping, reduced tooling costs, and the ability to manufacture complex shapes. However, challenges such as limited formability and quality issues persist, particularly in alloys like AA6061. Enhancing formability in AA6061 is crucial for expanding its applicability in various industries, including aerospace and automotive, where lightweight, high-strength materials are in demand [1]. Addressing these challenges through optimized process parameters can improve the efficiency, reliability, and versatility of ISF, making it a more viable manufacturing technique for complex components.

Sharma et al. delved into ISF effects on mechanical properties, focusing on incremental depth and tool diameter. Utilizing Digital Image Correlation (DIC) and texture analysis, they examined strain distribution and dislocation density. Incremental depth improved tensile strength, but larger tool diameters marginally reduced it due to altered tool movements, [2]. Alharbi investigated ultrasonic vibration's impact on AA6061-T6 alloy forming, finding varying amplitudes affecting forming force, thickness distribution, and accuracy. Higher amplitudes reduced force and deviation but led to thinning in critical regions [3].

Darzi et al. investigated the impact of temperature on SPIF for AA6061 alloy sheets from 25°C to 400°C, observing a significant enhancement in cone formability with elevated temperatures. They achieved a remarkable 44 mm depth for a truncated cone with a 65° wall angle, showcasing superior formability compared to cold ISF. Elevated temperatures facilitated plastic deformation, activating more slip planes, and significantly boosting formability, [4]. Seyyedi et al. compared Conventional hole flanging (CHF) and Incremental hole flanging (IHF) processes for AA6061-T6 sheets, finding CHF with a higher forming limit due to reduced damage, while IHF exhibited improved formability despite nonlinear stress and strain states, [5].

Ghaferi et al. explored enhancing formability and hardness of AA6061 alloy through various ISF heat treatment cycles: solid solution/SPIF/aging, solid solution/aging/SPIF, and annealing/SPIF/solid solution/aging. They found cold working of annealed sheets optimal for a 70° wall angle, doubling forming depth with a slight hardness increase, [6]. Zhan et al. proposed a two-stage Friction stir-assisted incremental sheet forming (FS-ISF) method

for aluminum alloys to achieve uniform microstructure and improved properties. Their model predicted uniform grain distribution post FS-ISF& reverse pass, enhancing material strength and ductility [7].
Zhan et al. further delved into FS-ISF, noting that higher speeds and smaller step-down increments improved formability, surface quality, and microstructure. Increased speed generated more frictional heat, softening the alloy for easier deformation and refining grain structure [8]. Tayebi et al. analyzed the formability and metallurgical properties of AA 6061 aluminum alloy sheets joined by Friction Stir Welding (FSW) and formed using ISF. Base and FSWed sheets were formed into conical shapes, revealing differences in strain and thickness distribution near welded areas, [9].
Tayebi et al. further examined the formability of dissimilar FSWed AA 6061 and AA 5083 blanks via ISF, noting similar formability between dissimilar FSWed and base metal sheets. Seyyedi et al. studied Incremental Hole Flanging (IHF) via ISF, applying the modified Mohr–Coulomb (MMC) criterion and a nonlinear damage accumulation rule to predict fractures in AA6061-T6 sheets during IHF. Their method accurately predicted fractures, surpassing traditional linear damage accumulation models [10]. Mirnia and Shamsari utilized the MMC3 criterion in Finate element (FE) simulations to predict ductile fracture in ISF, calibrated for AA6061-T6 alloy, underscoring the importance of considering non-proportional loading paths in fracture predictions, [11].
Mandaloi et. al. explored deformation machining (DM) for producing impeller blades from AA6061-T6 alloy, focusing on tool path development, forming strategies, and their impacts on forces, geometric accuracy, and surface roughness [12]. Vahdani et al. investigated Electric Hot Incremental Sheet Forming (EHISF) on various sheet metals, noting improvements in formability for Ti-6Al-4V and AA6061, influenced by lubricant type and electric current, [13]. Azpen et al. studied how process parameters affected surface roughness in FS-ISF, identifying optimal parameters for improved manufacturing efficiency, [14].
The literature review underscores the significance of ISF processes, particularly in enhancing the formability of AA6061 aluminum alloy sheets. However, existing studies reveal challenges such as limited formability and quality of the formed part. Thus, there is a compelling need for further research to systematically investigate and optimize the process parameters in a novel incremental sheet forming approach specific to AA6061 alloy. By varying parameters such as step depth, feed rate, spindle speed and tool diameter, this study aims to address existing limitations and enhance the formability of AA6061 sheets, contributing to the advancement of ISF technology and its practical applications in manufacturing complex components.

2. MATERIALS AND METHODOLOGY

A 1 mm thick sheet of AA6061 T6 having $150 * 150\ mm^2$ blank size was chosen to perform the ISF experiments due to its widespread use in automotive and aerospace industries, [1]. The chemical composition and mechanical properties of the material is mentioned in Table 1 & 2 respectively. A conical frustum having major diameter of 100 mm and wall angle (α) of 60° was formed on 3-axes CNC milling machine using spiral tool path generated through MATLAB© program as seen in Figure 1, [15]. A petroleum based synthetic oil was used as the lubricant on hemi-spherical tool profile [16]. All the experiments were performed until the crack formation and the depth at the crack formation was considered as the fracture forming depth. Taguchi design of experiments was followed with four process parameters, tool diameter (d) ranging from 6 mm to 14 mm, spindle speed (s) ranging from 500 rpm to 1400 rpm, step depth (Δz) ranging from 0.2 mm to 0.8 mm and feed rate (f) ranging from 250 mm/min to 1250 mm/min.

Table 1. Chemical composition of AA6061 T6 [17]

Material (%)	Mg	Si	Fe	Mn	Al
AA6061 T6	1.19	0.62	0.172	0.09	Balance

Table 2. Mechanical properties of AA6061 T6 [3]

Property	Values
Yield strength (MPa)	302
Ultimate tensile strength (MPa)	334
Elongation (%)	18
Hardness (HV)	130.98

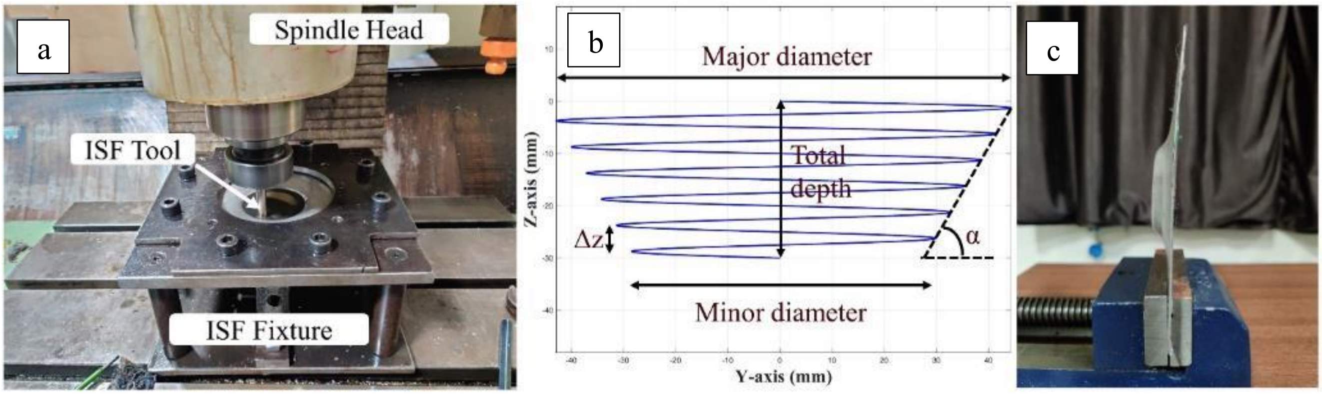

Fig. 1. (a) ISF set-up (b) Spiral tool path with geometric denotations and (c) formed sample

The range of these parameters were selected by trial experimentations and literatures [18], [19]. After the experimentations the statistical analysis was carried out to assess the performance of the design of the experiments using 4 factors at 3 levels following Taguchi's design. The impact of the individual process parameters along with their interaction effect on the fracture forming depth. Optimal process parameters were finalized based on the statistical analysis using MINITAB© and validation experiments were performed.

3. RESULTS AND DISCUSSION

The Table 3 shows the fracture forming depth at various process parameters. Each experiment was repeated thrice and the average values are reported. The results of these experiments are analyzed using different statistical techniques like ANOVA analysis and main effect plots considering higher the fracture forming depth better criterion.

Table 3. Experimental data on fracture forming depths for various process parameters

Sr. No.	Tool dimeter (mm)	Spindle speed (rpm)	Step depth (mm)	Feed rate (mm/min)	Avg. Fracture forming depth (mm)
1	6	500	0.2	250	10.393
2	6	1000	0.5	750	13.414
3	6	1400	0.8	1250	10.897
4	10	500	0.5	1250	9.268
5	10	1000	0.8	250	9.882
6	10	1400	0.2	750	9.91
7	14	500	0.8	750	13.426
8	14	1000	0.2	1250	10.352
9	14	1400	0.5	250	12.385

3.1. Effect of Tool diameter

The tool diameter plays a crucial role in determining the fracture forming depth in incremental forming processes. As the tool interacts with the workpiece, it induces material deformation through localized stretching and thinning. A larger tool diameter allows for greater contact area with the workpiece, facilitating more extensive material displacement [20]. This results in increased deformation and, consequently, deeper fracture forming depth as seen in experiment no. 7,8, 9. Conversely, a smaller tool diameter restricts the contact area and may lead to insufficient material flow, limiting the achievable fracture forming depth. At lower tool diameter, the material is prone to chipping as lesser contact area induces higher stresses in the material subsequently increasing the effective strain. The effective strain value exceeds the limiting strain, thus its easier for material to shear than form leading to chipping of the material, ultimately resulting in premature failure of the component as shown in Figure 2. This phenomenon is highly localized and depended on the material properties at that particular location, making the forming depth unpredictable. The higher shear loading is further confirmed by the tool breakage at 6 mm tool diameter as shown Figure 2(d).

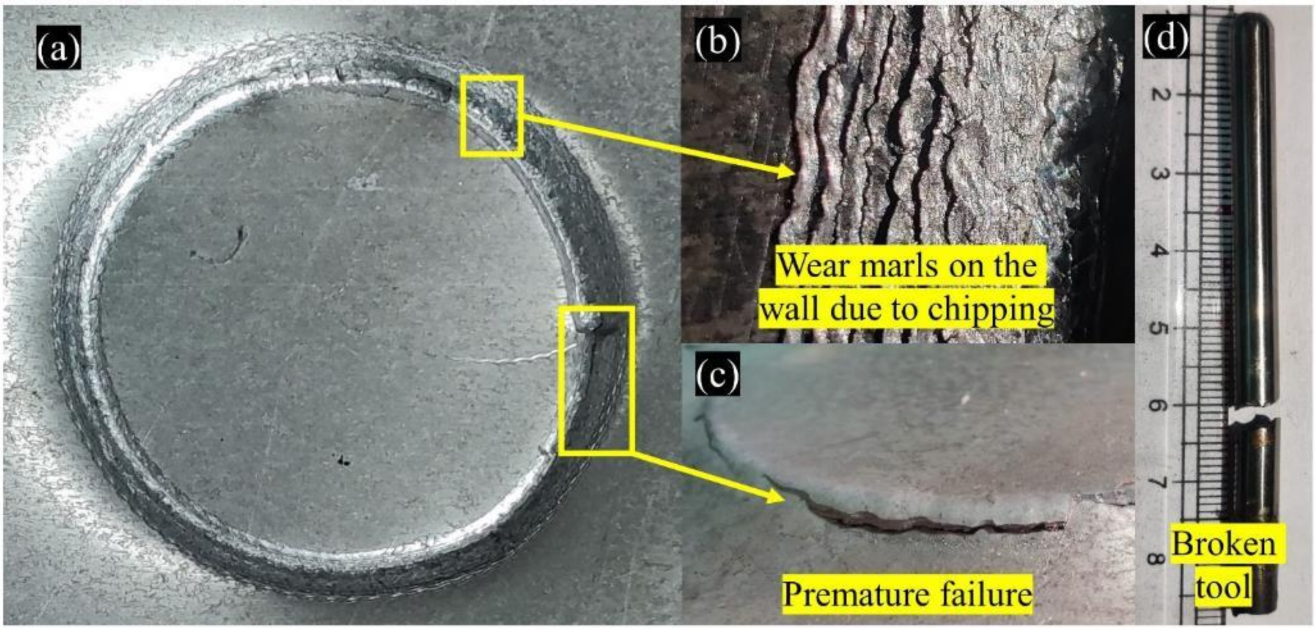

Fig. 2. (a) formed sample using 6 mm tool diameter, (b) wear marks due to chipping, (c) Crack formation and (d) broken 6 mm forming tool

Furthermore, the statistical analysis reveals significant effects of tool diameter on fracture forming depth. The ANOVA analysis demonstrates a highly significant F-value for tool diameter as shown Table 4, indicating its substantial impact on the response variable. Moreover, the main effect for means illustrates a non-linear trend in fracture forming depth with varying tool diameters. Initially, as the tool diameter increases, the fracture forming depth increases, reaching an optimal point before declining slightly and then increasing again as shown in Figure 4(a). A larger tool diameter allows for more extensive material deformation by providing a greater contact area with the workpiece. This facilitates enhanced material flow and displacement, leading to increased fracture forming depth. Increasing the tool diameter alters the distribution of strain across the workpiece [21]. A larger tool diameter can distribute strain more evenly, minimizing localized deformation and promoting deeper fracture forming as shown in Figure 3. Larger tool diameters offer better stability and stiffness during forming, reducing vibrations and tool deflection. This stability ensures more consistent and predictable deformation, contributing to higher fracture forming depth [22]. Hence, higher tool diameter is preferable to avoid chipping of the material and better formability.

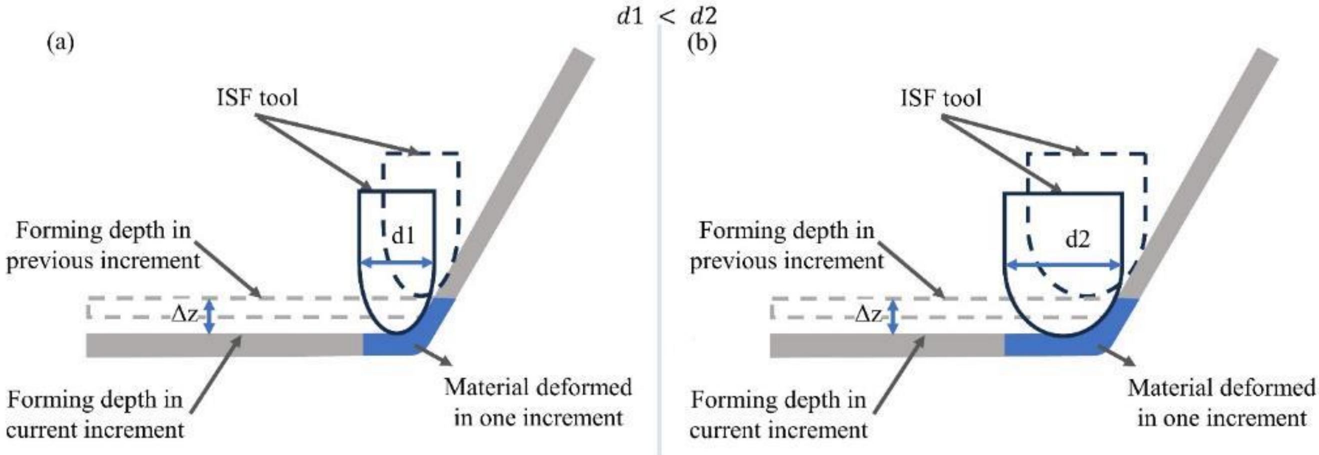

Fig. 3. Effect of tool diameter on the amount of material to be deformed in ISF process

Table 4. Analysis of Variance along with model summary

Analysis of Variance (ANOVA)					
Source	DF	Adj SS	Adj MS	F-Value	P-Value
Tool Dia	2	28.1463	14.0731	44.54	0.0000001
Spindle speed	2	0.1781	0.0891	0.28	0.7576418
Step depth	2	10.9383	5.4691	17.31	0.0000641
Feed rate	2	20.0635	10.0318	31.75	0.0000013
Error	18	5.6873	0.3160		
Total	26	65.0135			

Model summary			
S	R-sq	R-sq(adj)	R-sq(pred)
0.562106	91.25%	87.36%	80.32%

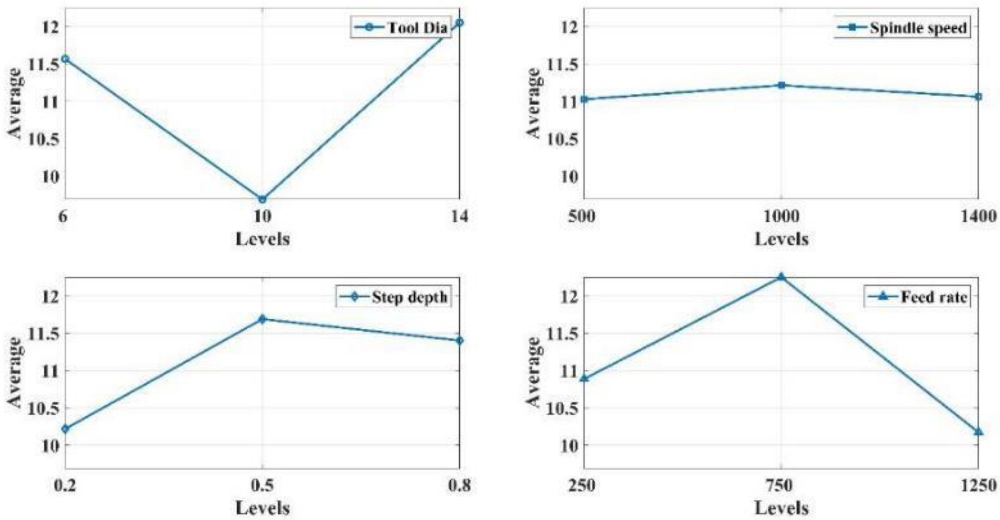

Fig. 4. Main effect plot of individual parameters on fracture forming depth

3.2. Effect of Step depth

Step depth influences fracture forming depth by controlling the amount of material deformation and the shape of the formed part. The step depth determines the distance the forming tool advances into the workpiece during each incremental step, directly impacting the depth of material displacement and deformation. A larger step depth results in greater material deformation and higher fracture forming depth, as more material is displaced with each step [24]. However, in the current observations, statistical analysis suggests that step depth has a significant effect on fracture forming depth. The main effect plot shows variations in fracture forming depth with changes in step depth, indicating its influence on the process as shown in Figure 4(c). This is further supported by a significant F-value for step depth in the ANOVA analysis presented in Table 4.

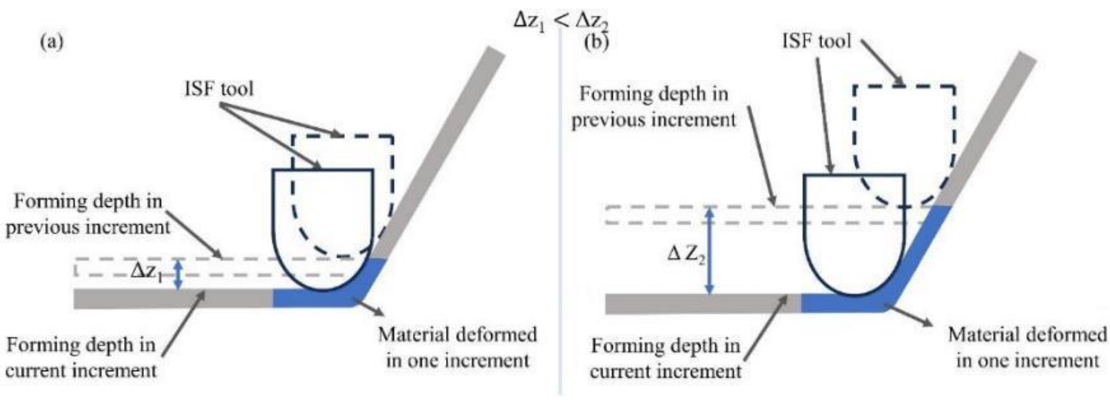

Fig. 5. Effect of step depth on the amount of material to be deformed

The increased fracture forming depth with increase in step depth can be justified by the work hardening of the material. AA6061-T6 exhibits significant work hardening behavior, where its strength increases as it undergoes plastic deformation. As the step depth increases, more material is deformed in a single step as shown in Figure 5, potentially leading to higher levels of work hardening. This increased work hardening can influence the material's ability to withstand further deformation, affecting fracture forming depth. However, with further increase in the step depth can increase the strength of AA6061, it may also lead to a reduction in ductility and potentially impact its toughness. This means that although work-hardened AA6061 may be stronger, it could also be more brittle and thus again reducing the fracture forming depth as seen in Figure 4(c) [25]. Thus, neither too low or too high step depth is not preferred especially in case of forming of AA6061.

3.3. Effect of Feed rate

Feed rate serves as a critical parameter in incremental forming processes, exerting a profound influence on fracture forming depth. As the forming tool traverses the workpiece, the feed rate dictates the pace at which material displacement and deformation occur per unit time. A higher feed rate typically leads to swifter tool movement, potentially resulting in escalated material flow and deformation rates, thus impacting fracture forming depth by modifying the extent and distribution of material deformation across the workpiece [26].
Statistical analyses of experimental data reveal the significant effect of feed rate on fracture forming depth. The ANOVA analysis yields a highly significant F-value for feed rate, indicating its substantial contribution to the variability in fracture forming depth as seen in Table 4. Additionally, the main effect for means demonstrates discernible disparities in fracture forming depth among different feed rate levels, corroborating the notable influence of feed rate on the forming process as shown in Figure 4(d). The feed rate directly influences the rate at which material undergoes displacement and deformation during forming. A higher feed rate fosters accelerated material flow and deformation, potentially culminating in augmented fracture forming depth. Conversely, a lower feed rate might curtail material flow and deformation, resulting in shallower fracture forming depth [27]. The observed impact of feed rate on fracture forming depth suggests the presence of an optimal feed rate for maximizing fracture forming depth. This optimal feed rate strikes a balance between material deformation rate and other process parameters, enabling the attainment of maximal fracture forming depth without compromising other facets of the forming process.

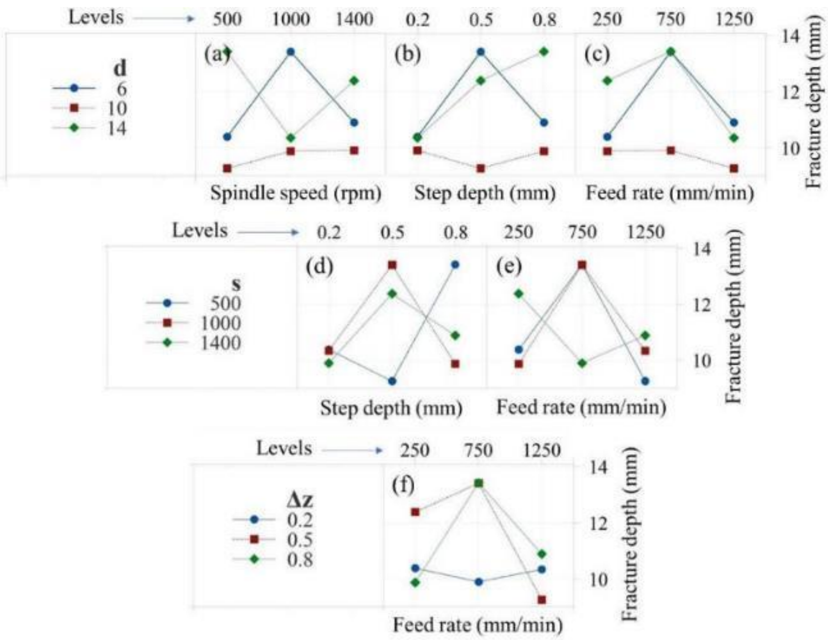

Fig. 6. Interaction plot of all the process parameters

3.4. Interaction effect

Figure 6(a) indicates a positive correlation between spindle speed and fracture depth across different tool diameters. As spindle speed increases, fracture depth also increases, suggesting a direct relationship between these parameters. This implies that higher spindle speeds lead to more extensive material deformation, potentially resulting in deeper fractures. Figure 6(b) illustrates an initial increase followed by a decrease in fracture depth with increasing step depth, consistent across all tool diameters. This trend suggests a nuanced relationship where higher step depths initially facilitate greater material deformation, leading to deeper fractures. However, beyond a certain point, excessively high step depths may lead to reduced fracture depth, due to increased brittleness. In Figure 6(c), as feed rate increases, fracture depth also increases, indicating that higher feed rates result in faster material displacement and deformation, leading to increased fracture depth.
Figure 6(d) depicts how the fracture forming depth first increases and then decreases with an increase in step depth across all spindle speeds. This suggests a complex relationship where moderate step depths lead to optimal

fracture forming depth, while excessively high step depths resulting in reduced fracture depth. While Figure 6(e) highlights a positive correlation between feed rate and fracture forming depth at different spindle speeds. Both parameters increase together, suggesting that higher feed rates, combined with higher spindle speeds, lead to more extensive material deformation and increased fracture forming depth. Figure 6(f) shows how increasing feed rate initially leads to a rise in fracture forming depth but then results in a decrease, across various step depth levels. This trend implies that while higher feed rates initially facilitate greater material deformation, excessively high feed rates may lead to reduced fracture depth. This provides the importance of carefully controlling the process parameters to achieve optimal fracture forming depth, especially considering the tool diameter, spindle speed, step depth and feed rate. From the current experimental investigation, higher tool diameter along with moderate spindle speed, step depth and feed rate are beneficial to achieve maximum fracture forming depth in ISF process.

3.5. Optimization of the fracture forming depth

From the ANOVA analysis (Table 4) tool diameter, feed rate and step depth are the most influential process parameters in that particular order, while spindle speed has no statistical influence on the fracture forming depth. The optimal combinations resulted from the statistical analysis is shown in Table 5. It also shows the predicted fracture depth and experimental fracture depth. A fracture depth of 14.75 mm was achieved at the optimal combination against the predicted 13.9 mm indicating the error % of only 5.76. This is further supported by the R^2 value of 91.25% and adjusted R^2 value of 87.36% as shown Table 4. This shows the robustness of the design and predictive model. The Figure 7(a) & 5(B) shows the appearance of the minor crack at 14.75 mm and crack propagation at 15 mm at the wall angle of 60°. The optimal experimental value is within the 95% prediction interval again validating the robustness of the predictive model. While the Figure 8 indicated the smooth surface obtained at the optimal parameters successfully avoiding the chipping of the material. The optimal combination of parameters, including a 14 mm tool diameter, 0.5 mm step depth, 750 mm/min feed rate, and 1000 rpm spindle speed, maximizes the material displacement and fracture forming depth while maintaining minimizing the risk of material failure. This combination balances the need for extensive material deformation with the limitations imposed by tool size, step depth, feed rate, and spindle speed, ensuring efficient forming while avoiding excessive strain rates or insufficient material flow.

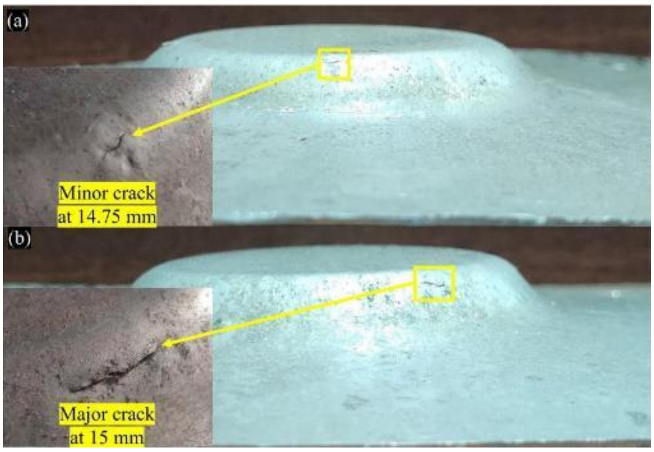

Fig. 7. Minor crack at 14.75 mm and crack propagation at 15 mm for the optimal solution

Table 5. Optimal solution and comparison of predicted vs experimental fracture depth

Tool Diameter (mm)	Spindle speed (rpm)	Step depth (mm)	Feed rate (mm/min)	Fracture depth Fit (mm)	Experimental fracture depth (mm)	% error
14	1000	0.5	750	13.9	14.75	5.76

Fig. 8. Smooth macrostructure at the optimal solution avoiding the chipping

4. CONCLUSIONS

This study systematically explored how varying parameters like tool diameter, spindle speed, step depth, and feed rate influence AA6061 formability in Incremental Sheet Forming. It highlighted the critical role of parameter control in enhancing formability. Following conclusions were drawn from the present study.
Tool diameter followed by the feed rate and step depth are significant parameters affecting the fracture forming depth as shown in Table 4 and Figure 4. While the spindle speed within the tested range does not affect the fracture forming depth significantly.
Tool diameter significantly influences fracture forming depth in incremental forming processes. Larger diameters facilitate greater material displacement, enhancing deformation and fracture depth, while smaller diameters can lead to material chipping and premature failure as seen in Figure 2.
The interaction between process parameters significantly affects fracture depth in incremental forming as shown in Figure 6. Optimal combinations, validated through statistical analysis and experimentation, demonstrate robustness in achieving desired fracture depths while avoiding material failure as shown in Table 5 and Figure 8.

Funding: This paper has received no external funding.
Conflicts of Interest: There is no conflict of interest.

REFERENCES

[1] Ajay, Mittal, R.K. (2020). *Incremental Sheet Forming Technologies: Principles, Merits, Limitations, and Applications* (1st ed.). CRC Press. doi: 10.1201/9780429298905

[2] M. Sharma, A. Bhattacharya, S. K. Paul, (2024), *Explicating tensile response of AA6061-T6 sheet post single point incremental forming: Two camera-DIC strain measurement and texture analysis*, *Mechanics of Materials*, 192, doi: 10.1016/j.mechmat.2024.104963.

[3] N. Alharbi, (2022), *Experimental study on designing optimal vibration amplitude in ultrasonic assisted incremental forming of AA6061-T6*, Engineering Science and Technology, an International Journal, 30, doi: 10.1016/j.jestch.2021.07.004.

[4] S. Darzi, M. Javad Mirnia, M. Elyasi, (2021), *Single-point incremental forming of AA6061 aluminum alloy at elevated temperatures*, The International Journal of Advanced Manufacturing Technology, 116(6), doi: 10.1007/s00170-021-07494-5/Published.

[5] S. E. Seyyedi, H. Gorji, M. J. Mirnia, M. Bakhshi-Jooybari, (2022), *Prediction of ductile damage and fracture in the single- and multi-stage incremental hole-flanging processes using a new damage accumulation law*, International Journal of Advanced Manufacturing Technology, 119, 7–8, 4757–4780, doi: 10.1007/s00170-021-08638-3.

[6] M. Ghaferi, M. J. Mirnia, M. Elyasi, H. Jamshidi Aval, (2019), *Evaluation of different heat treatment cycles on improving single point incremental forming of AA6061 aluminum alloy*, International Journal of Advanced Manufacturing Technology, 105, 1–4, 83–100, doi: 10.1007/s00170-019-04167-2.

[7] X. Zhan, D. An, J. Chen, (2022), *A novel two-stage friction stir-assisted incremental sheet forming method for uniform microstructure and enhanced properties in aluminum alloys*, Int J Mach Tools Manuf, 180, doi: 10.1016/j.ijmachtools.2022.103928.

[8] X. Zhan, W. Huang, D. Li, J. Chen, (2021), *An optimum process window to preferable microstructure distribution and improved macroscopic property for friction stir-assisted incremental aluminum alloy sheet forming*, The International Journal of Advanced Manufacturing Technology,115(11), doi: 10.1007/s00170-021-07194-0/Published.

[9] P. Tayebi, A. Fazli, P. Asadi, M. Soltanpour, (2021), *Formability study and metallurgical properties analysis of FSWed AA 6061 blank by the SPIF process*, SN Appl Sci, 3(3), doi: 10.1007/s42452-021-04378-x.

[10] P. Tayebi, A. Fazli, P. Asadi, M. Soltanpour, (2019), *Formability analysis of dissimilar friction stir welded AA 6061 and AA 5083 blanks by SPIF process*, CIRP J Manuf Sci Technol, 25, 50–68, doi: 10.1016/j.cirpj.2019.02.002.

[11] M. J. Mirnia, M. Shamsari, (2017), *Numerical prediction of failure in single point incremental forming using a phenomenological ductile fracture criterion*, J Mater Process Technol, 244, 17–43, doi: 10.1016/j.jmatprotec.2017.01.029.

[12] G. Mandaloi, A. Nagargoje, G. Banerjee, A. Gupta, P. Tandon, (2022), *Assessment of response parameters of the bending mode of deformation machining for manufacturing of impeller blades*, Journal of the Brazilian Society of Mechanical Sciences and Engineering, 44(11), doi: 10.1007/s40430-022-03811-5.

[13] M. Vahdani, M. J. Mirnia, M. Bakhshi-Jooybari, H. Gorji, (2019), *Electric hot incremental sheet forming of Ti-6Al-4V titanium, AA6061 aluminum, and DC01 steel sheets*, International Journal of Advanced Manufacturing Technology, 103(1–4), 1199–1209, doi: 10.1007/s00170-019-03624-2.

[14] Q. Azpen, H. Baharudin, S. Sulaiman, F. Mustapha, (2018), *Effect of process parameters on the surface roughness of aluminum alloy AA 6061T6 sheets in frictional stir incremental forming*, Advances in Production Engineering and Managemen*t*, 13(4), 405–416, doi: 10.14743/apem2018.4.299.

[15] S. Thibaud, R. Ben Hmida, F. Richard, P. Malécot,(2012), *A fully parametric toolbox for the simulation of single point incremental sheet forming process: Numerical feasibility and experimental validation*, Simul Model Pract Theory, 29(32–43), doi: 10.1016/j.simpat.2012.07.004.

[16] A. Dabwan, A. E. Ragab, M. A. Saleh, S. Anwar, A. M. Ghaleb, A. U. Rehman, (2020), *Study of the Effect of Process Parameters on Surface Profile Accuracy in Single-Point Incremental Sheet Forming of AA1050-H14 Aluminum Alloy*, Advances in Materials Science and Engineering, 2020, doi: 10.1155/2020/7265941.

[17] G. Chudasama, S. Wanare, V. Kalyankar, (2023), *Influence of substrate surface roughness on push-off strength for friction surfacing of low carbon steel with aa6061-t6 aluminium alloy*, International Journal of Modern Manufacturing Technologies, 15(2), 56–62, 2023, doi: 10.54684/ijmmt.2023.15.2.56.

[18] S. Marathe, H. Raval, (2020), *Simulation study on single point incremental forming of tailor welded blanks*, International Journal of Modern Manufacturing Technologies, 12(2), 93–101.

[19] M. Shalin, M. Hiten, (2018), *Experimental Analysis on Effect of Tool Transverse Feed, Tool Rotational Speed and Tool Pin Profile Type on Weld Tensile Strength of Friction Stir Welded Joint of AA 6061*, Mater Today Proc, 5(1), 487–493, doi: 10.1016/j.matpr.2017.11.109.

[20] A. Kumar, V. Gulati, P. Kumar, H. Singh, (2019), *Forming force in incremental sheet forming: a comparative analysis of the state of the ar*t, Journal of the Brazilian Society of Mechanical Sciences and Engineering, 41(6), Springer Verlag, doi: 10.1007/s40430-019-1755-2.

[21] G. Centeno, I. Bagudanch, A. J. Martínez-Donaire, M. L. García-Romeu, C. Vallellano, (2014), *Critical analysis of necking and fracture limit strains and forming forces in single-point incremental forming*, Mater Des, 63, 20–29, doi: 10.1016/j.matdes.2014.05.066.

[22] I. Bagudanch, M. L. Garcia-Romeu, G. Centeno, A. Elías-Zúñiga, J. Ciurana, (2015), *Forming force and temperature effects on single point incremental forming of polyvinylchloride*, J Mater Process Technol, 219, 221–229, 2015, doi: 10.1016/j.jmatprotec.2014.12.004.

[23] A. Kumar, V. Gulati, and P. Kumar, (2018), *Investigation of Surface Roughness in Incremental Sheet Forming*, Procedia Computer Science, Elsevier B.V., pp. 1014–1020. doi: 10.1016/j.procs.2018.07.074.

[24] G. Ambrogio, I. Costantino, L. De Napoli, L. Filice, L. Fratini, M. Muzzupappa, (2004), *Influence of some relevant process parameters on the dimensional accuracy in incremental forming: A numerical and experimental investigation*, J Mater Process Technol, 153–154 (1–3), 501–507, doi: 10.1016/j.jmatprotec.2004.04.139.

[25] J.-C. Li, L. I. Chong, Z. Tong-Gui, (2012), *Thickness distribution and mechanical property of sheet metal incremental forming based on numerical simulation*, Transactions of Nonferrous Metals Society of China, 22, 54-60, doi: 10.1016/S1003-6326(12)61683-5.

[26] G. Hussain, L. Gao, Z. Y. Zhang, (2008), *Formability evaluation of a pure titanium sheet in the cold incremental forming process*, International Journal of Advanced Manufacturing Technology, 37(9–10), 920–926, doi: 10.1007/s00170-007-1043-7.

[27] M. Ham, J. Jeswiet, (2006), *Single Point Incremental Forming and the Forming Criteria for AA3003*, *CIRP Annals,* 55, 241-244, doi: 10.1016/S0007-8506(07)60407-7.

Received: September 9th, 2024 / Accepted: December 15th, 2024 / Paper available online: December 20, 2024 ©
International Journal of Modern Manufacturing Technologies.